STEREOPHOTOCLINOMETRY TERRAIN GENERATION SUPPORTING AUTONOMOUS OSIRIS-REX TOUCH-AND-GO SAMPLE COLLECTION.

E. E. Palmer[1]*, J. R. Weirich[1], K. Lopez[1], O. S. Barnouin[2], M. G. Daly[3], R. Gaskell[1], C. Miller[4], R. Olds[4], C. Mario[5], C. Norman[4], D. A. Lorenz[6] and D. S. Lauretta[7], [1]PSI, Tucson, AZ, USA, (epalmer@psi.edu), [2]JHUAPL, Laurel, MD, USA, [3]York U., Toronto, Ontario, Canada, [4]Lockheed Martin Space, Littleton, CO, USA, [5]Draper, Cambridge, MA, USA , [6]NASA GSFC, Greenbelt, MD, USA, [7]LPL, Univ. of Arizona, Tucson, AZ, USA.

Introduction: The OSIRIS-REx mission [1] is bringing back a sample from the surface of asteroid Bennu. To acquire the sample, the spacecraft autonomously navigated to a site on Bennu's surface called Nightingale to conduct the "touch-and-go" (TAG) sample collection maneuver [2]. The surface of Bennu was significantly rougher and more hazardous than expected. The largest sample collection site that could support safe operations was only ~8 meters in radius, rather than the expected 25 m radius region that was expected. The navigation performed extremely well, allowing for a safe and successful sample collection from Bennu's hazard-covered surface.

The spacecraft began its descent to the surface from a 1-km-altitude terminator orbit with a single burn. The autonomous navigation system, called Natural Feature Tracking (NFT), used images taken by one of the navigational cameras with a wide field of view to calculate how closely the spacecraft's actual position matched the desired position, [2,3].

As the spacecraft descended, it performed these checks numerous times so that when it reached Checkpoint (~120 m above the surface), it would have sufficient information to calculate a small course correction. The spacecraft repeated this before Match-point (~50 m above the surface) [1].

Because there is always a small amount of error in a spacecraft burn, the spacecraft took several more images that were fed into the NFT system. This final check was to ensure that the spacecraft's final trajectory, which was fully ballistic at this point, was within the required limits after the last burn.

NFT was able to determine the spacecrafts' trajectory to within 1 m during descent. The final touchdown point of the spacecraft was estimated at 0.7 m from the selected target of the TAG event, indicating that the two course corrections performed excellently.

NFT Feature Generation: We created a database of 225 features to support NFT navigation to both the primary sample collection site, Nightingale, and the backup site, Osprey [5]. Each feature is a small digital terrain model (DTM) generated using stereophotoclinometry (SPC) that is 125×125 pixels in size and has a ground sample distance (GSD) that closely matches the camera pixel scale to which it is compared. Each feature must be accompanied by both terrain geometry and albedo so that a model can be rendered to match the navigation images (Fig. 1).

The highest-resolution NFT features used the images from the Detailed Survey mission phase with 5 cm/pixel as a baseline. To that data, we added image data from the Reconnaissance mission phase with 2 cm/pixel (Recon A) and 1 cm/pixel (Recon B). Although not an imaging requirement for an SPC DTM, the mission collected Recon C data at 0.25 cm over much of both sample collection sites. We used this additional data to improve the DTM of each feature, which helped the feature obtain a higher correlation score and detection probability. This was important because, during the descent to the surface, NFT would be taking data in spacecraft and solar geometries not represented in previous images. As such, the renderings of those DTMs would be based on extrapolation of the DTM created from other images rather than directly matching what we had previously acquired.

During the generation of the feature database, we created a series of regions focused around each feature in which the resolution was generated at higher and higher GSD. We covered a feature region with a grid of small DTMs (maplets) that were 18×18 m at 6 cm GSD. Using this new terrain, we made a grid of 2-cm-GSD maplets over a 6×6 m region. Each starting DTM came from the 6-m DTMs that are sufficient for aligning images. Then the new image data allowed 2-cm DTM data to be calculated. We continued this "step down" technique to generate a 3-m region at 1 cm GSD, and then again for a 1.5-m region at 0.5 cm GSD.

We generated features with a GSD from 16 cm down to 0.75 cm for the Nightingale site and 0.5 cm for the Osprey site. The specific resolution was based upon the flight profile, how fast the spacecraft descended in different gravity regimes, and when the images were needed.

In generating the features, we processed maplets until they reached a GSD significantly higher than requested in order to extract as much sub-pixel information from the images as possible. Thus, the highest resolution of the maplets were generated at requested GSD divided by 2 — meaning that if the navigation feature was going to be used for an image that had a pixel size of 1 cm, we generated maplets at 0.5 cm GSD. Then we downsampled the data to make a more accurate navigation feature at 1 cm than can be done without this technique.

Discussion: Features that seem useful to humans are seldom effective for computer vision based autonomous navigation. Large, steeply sloped boulders, for example, have been shown to be poor features for computer vision algorithms [7, 8]. Because of our extensive testing, we realized that terrains with smaller features, such as small craters, smooth patches, or strong localized albedo features, provided the highest correlation scores. Having features without significant shadows is important because small error on the absolute height of a boulder results in a large error in the length of its shadow.

Additionally, it became clear during testing that foreshortening with high emission angles can be a problem. NFT features that were used when the emission angle was greater than 50° did not perform nearly as well as those at 45° or less. Additionally, emission angles greater than 60° are very difficult to use effectively. Although SPC can use images with emission angles of 70° or higher, rendering of the terrain is difficult at these extremes.

Feature Performance: In addition to the strong performance of the autonomous navigation previously mentioned, the NFT feature database also performed very well. From the start of the sample collection operation, a total of 30 images were processed by the spacecraft. For each image NFT successfully achieved the detection of all of the features that had been assigned to that image. There were 123 feature detections with an average correlation score of 0.726. Only three feature detections that had correlation scores in the marginal range between 0.50-0.60 and most features were above 0.7. There were 21 feature detections that were above 0.8 with the highest correlation score of 0.856. There were no false positives (locating the wrong location — the worst-case scenario), no false negatives (not locating the valid location) , and no match below correlate threshold (finding the right location, but a correlation score that is too low).

Conclusion: Our SPC-based method was able to generate an exceptional database of NFT features that enabled successful sample collection at the Nightingale site within 1 m of the targeted point. This demonstrates that SPC can provide a strong and stable tool for landmark navigation. It is especially useful in operations in which there is low gravity when Doppler navigation becomes limited.

Acknowledgments: This material is based upon work supported by NASA under Contract NNM10AA11C issued through the New Frontiers Program. We are grateful to the entire OSIRIS-REx Team for making the encounter possible. We also acknowledge the exceptional work of the entire OSIRIS-REx GN&C team at Lockheed Martin Space that provided extensive support in developing the procedures, techniques and evaluation of these features.

References: [1] Lauretta, D. S., et al., 2017. Space Sci. Rev. 212, 925–984. [2] Olds, R., et al., 2015. AAS GNC 15-124. [3] Lorenz, D. A., 2017. IEEE Aerospace Conference. DOI: 10.1109/AERO.2017.7943684. [4] Gaskell, R. W., 2008. MAPS, 43, 1049–61. [5] Palmer, E., 2019. DPS. [6] Mario, C., et al., 2020. Am Astro Soc Conf. 20-087, 765-776. [7] Mario, C., Debrunner, C., 2016. Am Astro Soc Conf. 16-087. 1-12.

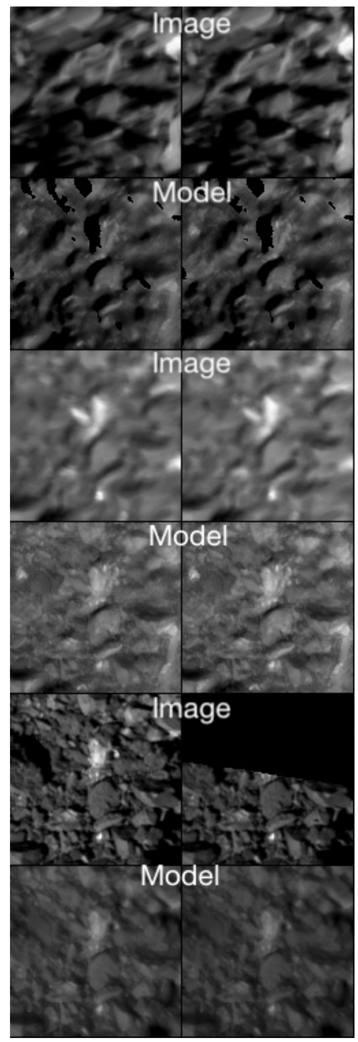

Figure 1. Examples of source images and the corresponding modeled features. The odd rows are the source images, orthorectified with Bennu north (+z) up. The even rows show the DTM rendered in the same illumination conditions as its corresponding image.